A Study on the Plane Couette Flow Using Micropolar Fluid Theory

Youn-Jea Kim*, Tae-An Kim
School of Mechanical Engineering, SungKyunKwan University, 300 CheonCheon-dong, Suwon 440-746, Korea

An analysis of the plane Couette flow between two parallel plates of a viscous, incompressible, micropolar fluid is presented. Especially, the effects of non-zero values of the micro-gyration boundary condition coefficient and pressure gradient on the flow fields are studied. Numerical results show that the micropolar parameter was found to have much more of an impact on the flow behaviors. It is also observed that the micro-gyration boundary condition coefficient influenced on the coefficients of skin friction and couple stress due to its different effect on the surface stress.

Key Words : Couette Flow, Micropolar Fluid, Micro-Gyration, Skin Friction, Couple Stress

Nomenclature

C_f : Skin friction coefficient
C_w : Couple stress coefficient
h : Height of microchannel
M_w : Couple stress
m : Model parameter
n : Micro-gyration boundary condition coefficient $(0 \leq n \leq 1)$
U_o : Scale of the referenced velocity
u, v : Longitudinal and transverse components of velocity vector, respectively
x, y : Distances along and perpendicular to the plate, respectively

Greek symbols

β : Dimensionless viscosity ratio
γ : Spin gradient viscosity
ρ : Fluid density
ξ : Mean free path
Λ : Coefficient of gyro-viscosity
τ_w : Shear stress
μ : Fluid dynamic viscosity
ω : Angular velocity vector

Superscript

$*$: Dimensional properties

* Corresponding Author,
E-mail : yjkim@skku.edu
TEL : +82-31-290-7448; **FAX** : +82-31-290-5849
School of Mechanical Engineering, SungKyunKwan University, 300 CheonCheon-dong, Suwon 440-746, Korea. (Manuscript **Received** December 12, 2002; **Revised** December 19, 2003)

1. Introduction

In order to design and fabricate microfluidic devices effectively, fluid flow behavior on the microscale must be clearly understood. In the last decades a number of studies have appeared in the literature on the flow of a viscous, incompressible fluid between two parallel plates. An exact solution of the Navier-Stokes equations for the plane Couette flow between two parallel plates is well known (Schlichting, 1979).

Experiments show that when the dimensions of the channels are in the μm-range, the measured data are different from those predicted by Navier-Stokes equations (Jiang et al., 1995; Yager and Brody, 1996). Discrepancies concern flow characteristics, such as, volumetric flowrate, average velocity, pressure drop and Darcy friction factor for incompressible fluids, flowing through microchannel. In addition, experimental observations show that the fluid viscosity close to the channel wall is higher (50-80%) than the bulk viscosity of

the fluid (Forcada and Mate, 1993).

In the theory of micropolar fluids, originated by Eringen (1964), both the effect of couple stresses and the microscopic effects arising from local structure and micro-rotation of the fluid element are simultaneously taken into account.

Previous research has indicated that the micropolar fluid model may provide a better agreement with the experimental data for microfluidic devices than the Navier-Stokes theory (Papautsky, 1999). In addition, the experiments and theoretical estimations indicate, that for real fluid flows the micropolar effects are important if the height of the channel is comparable to the dimensions of the particles of the fluid. On the other hand, when the dimensions of the container approach the dimensions characteristic for the molecular structure of the medium inside (i.e., mean free path), the assumption of continuum seems not to be justified.

In the present work we extend the use of micropolar fluid theory to examine fluid behaviors in a plane Couette flow. Especially, we consider the effect of non-zero values of the micro-gyration boundary condition coefficient on the variation of skin friction and couple stress at the plates with respect to given flow conditions.

2. Formulation of the Problem

In a micropolar fluid, the local fluid elements are allowed to undergo only rigid rotations without stretch. A coordinate system is introduced with its origin on the lower stationary plate lying horizontally on the x^*z^*-plane. The governing equations for micro-continuum fluid flow can be simplified by considering isothermal, incompressible microfluids, with no body forces, and steady-state flow (Ariman et al., 1973):

$$\frac{\partial u^*}{\partial x^*}+\frac{\partial v^*}{\partial y^*}=0 \tag{1}$$

$$u^*\frac{\partial u^*}{\partial x^*}+v^*\frac{\partial u^*}{\partial y^*} =-\frac{1}{\rho}\frac{\partial p^*}{\partial x^*}+\frac{1}{\rho}(\mu+\Lambda)\left(\frac{\partial^2 u^*}{\partial x^{*2}}+\frac{\partial^2 u^*}{\partial y^{*2}}\right)+\frac{\Lambda}{\rho}\frac{\partial \omega^*}{\partial y^*} \tag{2}$$

$$u^*\frac{\partial v^*}{\partial x}+v^*\frac{\partial v^*}{\partial y^*} =-\frac{1}{\rho}\frac{\partial p^*}{\partial y^*}+\frac{1}{\rho}(\mu+\Lambda)\left(\frac{\partial^2 v^*}{\partial x^{*2}}+\frac{\partial^2 v^*}{\partial y^{*2}}\right)-\frac{\Lambda}{\rho}\frac{\partial \omega^*}{\partial x^*} \tag{3}$$

$$u^*\frac{\partial \omega^*}{\partial x^*}+v^*\frac{\partial \omega^*}{\partial y^*} =-\frac{2\Lambda}{\rho j^*}\omega^*+\frac{\gamma}{\rho j^*}\left(\frac{\partial^2 \omega^*}{\partial x^{*2}}+\frac{\partial^2 \omega^*}{\partial y^{*2}}\right)+\frac{\Lambda}{\rho j^*}\left(\frac{\partial v^*}{\partial x^*}-\frac{\partial u^*}{\partial y^*}\right) \tag{4}$$

where x^* and y^* are the dimensional distances longitudinal and perpendicular to the plate, respectively. u^* and v^* are the components of dimensional velocities along x^* and y^* directions, respectively. ρ is the density, μ is the translational viscosity, Λ is the coefficient of gyro-viscosity (or vortex viscosity), j^* is the micro-inertia density, ω^* is the component of the angular velocity vector normal to the x^*y^*-plane, and γ is the spin-gradient viscosity which gives some relationship between the coefficients of viscosity and micro-inertia (Ahmadi, 1976; Kim, 1999):

$$\gamma=\left(\mu+\frac{\Lambda}{2}\right)j^*=\mu j^*\left(1+\frac{1}{2}\beta\right) \tag{5}$$

where β denotes the dimensionless viscosity ratio, defined as follows:

$$\beta=\frac{\Lambda}{\mu} \tag{6}$$

We consider a plane Couette flow of a viscous, incompressible, micropolar fluid between two parallel plates of distance h apart. The upper plate is given in uniform motion u_p^* along the x^*-axis. We also assume that a pressure gradient becomes constant along the streamwise direction.

Under these assumptions, the appropriate boundary conditions for the velocity and micro-rotation fields are

$$u^*=0,\ \omega^*=-n\frac{\partial u^*}{\partial y^*} \text{ at } y^*=0 \tag{7}$$

$$u^*=u_p^*,\ \omega^*=-n\frac{\partial u^*}{\partial y^*} \text{ at } y^*=h \tag{8}$$

Here the boundary condition for micro-rotation variable ω^* describes its relationship with the surface stress. In this equation, the boundary condition coefficient (n) is a number between 0

and 1 that relates the micro-gyration vector to the shear stress. The value $n=0$ corresponds to the case where the particle density is sufficiently large so that microelements close to the wall are unable to rotate. The value $n=0.5$ is indicative of weak concentrations, and when $n=1$ flows are believed to represent turbulent boundary layers (Rees and Bassom, 1996).

Ahmadi (1976) demonstrated that the micro-rotation density is directly proportional to the square of the length scale of a sensitive volume element. This length scale is defined as the smallest volume for which average quantity, such as velocity, density, gyration, has statistical meaning. In addition, we introduce the relation of mean free path (ξ) to the microstructure characteristic length (l) with the help of model parameter m as follows:

$$m=\frac{l}{\xi} \tag{9}$$

Since the microstructure length is less than the flow characteristic length (in this study the height of the microchannel, h), we may have the following relation, using Knudsen number ($Kn=\xi/h$):

$$Kn\leq\frac{1}{m} \tag{10}$$

We now introduce the following dimensionless variables:

$$x=\frac{x^*}{h},\ y=\frac{y^*}{h},\ u=\frac{u^*}{U_o},\ v=\frac{v^*}{U_o},$$
$$U_p=\frac{u_p^*}{U_o},\ \omega=\frac{h}{U_o}\omega^*,\ j=\frac{j^*}{h^2}=\frac{m^2}{10},\ p=\frac{p^*-p_\infty}{\rho U_o^2} \tag{11}$$

in which U_o is a scale of the referenced velocity.

After applying the locally fully developed flow assumption, the terms $\partial/\partial x$ will be vanished. However, we consider the case of a constant pressure gradient in the direction of fluid flow. The partial differential operator $\partial/\partial y$ is identical to the ordinary differential operator d/dy. Then, the above governing equations reduce to the following dimensionless form:

$$-\frac{dp}{dx}+\frac{1+\beta}{\mathrm{Re}}\frac{\partial^2 u}{\partial y^2}+\frac{\beta}{\mathrm{Re}}\frac{\partial\omega}{\partial y}=0 \tag{12}$$

$$-\frac{20\beta}{m^2}\omega+\left(1+\frac{\beta}{2}\right)\frac{\partial^2\omega}{\partial y^2}-\frac{10\beta}{m^2}\frac{\partial u}{\partial y}=0 \tag{13}$$

where $\mathrm{Re}=\rho U_o h/\mu$ is the Reynolds number.

In addition, the boundary conditions (7) and (8) may be written as the following dimensionless form:

$$u=0,\ \omega=-n\frac{\partial u}{\partial y}\ \text{at}\ y=0 \tag{14}$$

$$u=U_p,\ \omega=-n\frac{\partial u}{\partial y}\ \text{at}\ y=1 \tag{15}$$

The solutions of Eqs. (12)-(13) with satisfying boundary conditions (14) and (15) are given by

$$\omega=C_1\left[e^{\lambda y}-\frac{1+(1-n)\beta}{(1-2n)(1+\beta)}\right]+C_2\left[e^{-\lambda y}-\frac{1+(1-n)\beta}{(1-2n)(1+\beta)}\right]-\frac{\mathrm{Re}}{2+\beta}\frac{dp}{dx}y \tag{16}$$

$$u=\frac{C_1}{1+\beta}\left\{\frac{\beta}{\lambda}(1-e^{\lambda y})+\frac{2[1+(1-n)\beta]}{(1-2n)}y\right\}-\frac{C_2}{1+\beta}\left\{\frac{\beta}{\lambda}(1-e^{-\lambda y})-\frac{2[1+(1-n)\beta]}{(1-2n)}y\right\}+\frac{\mathrm{Re}}{2+\beta}\frac{dp}{dx}y^2 \tag{17}$$

Here the coefficients C_1 and C_2 are defined as follows:

$$C_1=\frac{1}{k_1}\left[-(1+\beta)U_p(e^{-\lambda}-1)+\frac{1+\beta}{2+\beta}\cdot\mathrm{Re}\frac{dp}{dx}\cdot b_1\right] \tag{18}$$

$$C_2=\frac{1}{k_1}\left[(1+\beta)U_p(e^{\lambda}-1)+\frac{1+\beta}{2+\beta}\cdot\mathrm{Re}\frac{dp}{dx}\cdot b_2\right] \tag{19}$$

where

$$\lambda=\frac{1}{m}\sqrt{\frac{20\beta}{1+\beta}} \tag{20}$$

$$k_1=\frac{2\lambda[1+(1-n)\beta]}{(1-2n)\beta}(e^{\lambda}-e^{-\lambda})-2(e^{\lambda}+e^{-\lambda})+4 \tag{21}$$

$$b_1=(e^{-\lambda}-1)\left(1+\frac{1-2n}{1+\beta-n\beta}\right)+\frac{2\lambda}{\beta}(1-2n) \tag{22}$$

$$b_2=(e^{\lambda}-1)\left(\frac{1-2n}{1+\beta-n\beta}-1\right)-\frac{2\lambda}{\beta} \tag{23}$$

The wall shear stress can be written as

$$\tau_w^*=\left[(\mu+\Lambda)\frac{\partial u^*}{\partial y^*}+\Lambda\omega^*\right]_{y^*=0,h}=\frac{\mu U_0}{h}[1+(1-n)\beta]\cdot\left.\frac{\partial u}{\partial y}\right|_{y=0,1} \tag{24}$$

Then, the coefficients of shear stress at the lower and upper plates are given by

$$C_f=\frac{2\tau_w^*}{\rho U_o^2}=\frac{2}{\mathrm{Re}}[1+(1-n)\beta]\cdot\left.\frac{\partial u}{\partial y}\right|_{y=0,1}$$
$$=\begin{cases}\dfrac{2}{\mathrm{Re}}\dfrac{(2+\beta)\cdot[1+(1-n)\beta]}{(1-2n)(1+\beta)}\cdot(C_1+C_2) & (\textit{lower plate})\\ \dfrac{2[1+(1-n)\beta]}{\mathrm{Re}}\cdot\left[\dfrac{2[1+(1-n)\beta]}{(1-2n)(1+\beta)}(C_1+C_2)\right. & \\ \left.-\dfrac{\beta}{1+\beta}(C_1e^{\lambda}+C_2e^{-\lambda})+\dfrac{2\mathrm{Re}}{2+\beta}\dfrac{dp}{dx}\right] & (\textit{upper plate})\end{cases} \quad (25)$$

The couple stress at the plates may be written as

$$M_w=\gamma\left.\frac{\partial\omega^*}{\partial y^*}\right|_{y^*=0,h} \quad (26)$$

Then, the coefficient of couple stress at the plates can be calculated as

$$C_w=\frac{M_w h^2}{\gamma U_o}=\left.\frac{\partial\omega}{\partial y}\right|_{y=0,1}$$
$$=\begin{cases}\lambda(C_1-C_2)-\dfrac{\mathrm{Re}}{2+\beta}\dfrac{dp}{dx} & (\textit{lower plate})\\ \lambda(C_1e^{\lambda}-C_2e^{-\lambda})-\dfrac{\mathrm{Re}}{2+\beta}\dfrac{dp}{dx} & (\textit{upper plate})\end{cases} \quad (27)$$

3. Results and Discussion

The effects of non-zero values of micro-gyration boundary condition coefficient and pressure gradient on the flow field and skin friction have been formulated in the preceding sections. This enables us to carry out the numerical computations for the velocities with various values of the flow conditions and fluid properties, m, n, β, Up, Re, and dp/dx, which are listed in the figure captions.

The effects of various values of the micropolar parameter β on the streamwise and micro-rotational velocities are shown in graphically in Fig. 1. It is seen that the translational velocity profiles are flatten as the β-parameter increases. The reason is that as a portion of the vorticity is used in producing micro-rotation, the presence of the micropolar elements has contributed to the retardation of the flow. As shown in Fig. 1(b), furthermore, the magnitude of peak values of the micro-rotational velocity is located near the upper plate. However, its maximum value increases initially and then decreases as the β-parameter increases. From these results we may deduce that the critical value of the viscosity ratio exists on the micro-rotational velocity.

Slight variation of the translational velocity and micro-rotational velocity profiles across the channel with different boundary condition coefficient (n) is observed in Fig. 2. The translational velocity profile shows an increasing nature as the n-parameter increases. However, the micro-rotational velocity profiles do not show consistent variations. In order to elucidate the

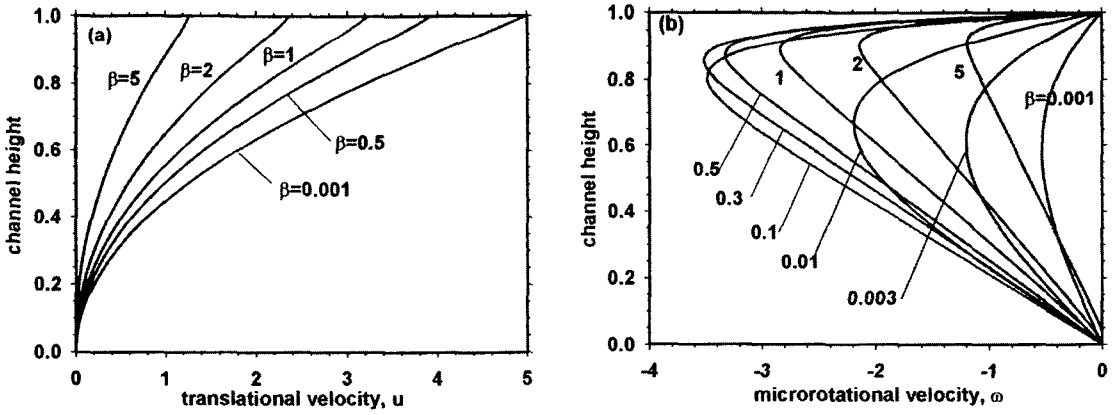

(a) Translational velocity (b) Micro-rotational velocity

Fig. 1 Effects of micropolar parameter β on velocity profiles for $n=0$, $m=0.1$, $Up=0.1$, $\mathrm{Re}=10$ and $dp/dx=1$

physical reasons for such a behavior, the variations of the skin friction and couple stress coefficients at the upper plate for Re=10, Up=0.1 and dp/dx=1 with different values of m, n and β are prepared in Table 1. Numerical results show that the relationship between the material constants to the flow coefficients may need to be further examined, as well as the parameter (n) in the boundary condition.

For the case of the particle density is sufficiently large close to the wall (n=0), velocity profiles for different values of the characteristic length ratio (m) are shown in Fig. 3. It is observed that with increasing value of m, the magnitude of translational velocity at the upper plate is reduced. In addition, as given in Table 1, the magnitude of the micro-rotational velocity distribution across the channel decreases as the m-parameter increases.

Figure 4 illustrates the distribution of stream-

Table 1 Variations of the skin friction and couple stress coefficients at the upper plate for Re=10, Up=0.1 and dp/dx=1

m	n	β	C_f	C_w	m	n	β	C_f	C_w
0.05	0.0	0.0001	1.9999	1.2669	0.5	0.0	0.0001	1.9989	0.0133
		0.01	1.9999	39.30			0.01	1.9936	1.2431
		0.1	1.9990	123.64			0.1	1.9929	8.1577
		0.5	1.9960	202.25			0.5	1.9673	16.32
		1.0	1.9925	206.69			1.0	1.9190	16.90
		5.0	1.9527	112.46			5.0	1.4794	7.20
	0.4	0.0001	1.2144	−4.6054		0.4	0.0001	−6.9340	−4.4340
		0.01	2.0000	−3.2024			0.01	1.1999	−4.5836
		0.1	2.0123	0.5153			0.1	1.8749	−4.2622
		0.5	2.0561	5.2952			0.5	1.9743	−3.2856
		1.0	2.0934	6.7887			1.0	1.9689	−2.7043
		5.0	2.1750	4.5651			5.0	1.6770	−1.7616
	1.0	0.0001	0.0361	−0.5279		1.0	0.0001	−20.33	−4.5528
		0.01	1.9773	39.70			0.01	0.0036	−0.5384
		0.1	1.8028	136.02			0.1	1.4976	8.9238
		0.5	1.1877	303.57			0.5	1.0706	24.91
		1.0	0.6533	413.87			1.0	0.5450	34.91
		5.0	−0.8411	674.98			5.0	−0.7522	53.13
0.1	0.0	0.0001	1.9998	0.3288	1.0	0.0	0.0001	1.9970	0.0033
		0.01	1.9999	17.17			0.01	1.9820	0.3190
		0.1	1.9994	59.43			0.1	1.9650	2.5221
		0.5	1.9939	98.96			0.5	1.9122	6.0581
		1.0	1.9849	101.28			1.0	1.8112	6.3312
		5.0	1.9040	54.11			5.0	0.8270	1.0991
	0.4	0.0001	0.2691	−4.5392		0.4	0.0001	−15.89	−4.4172
		0.01	1.9811	−4.0907			0.01	0.2384	−4.5161
		0.1	2.0094	−2.1499			0.1	1.4983	−4.4141
		0.5	2.0482	0.5280			0.5	1.7689	−3.7208
		1.0	2.0801	1.5174			1.0	1.7549	−3.2026
		5.0	2.1210	1.0627			5.0	1.0585	−2.1089
	1.0	0.0001	−2.3268	−2.7639		1.0	0.0001	−42.71	−4.7763
		0.01	1.9293	17.34			0.01	−2.3672	−2.7694
		0.1	1.7963	65.39			0.1	0.6738	1.9328
		0.5	1.1758	148.67			0.5	0.7768	9.6709
		1.0	0.6403	203.08			1.0	0.3579	14.37
		5.0	−0.8268	326.34			5.0	−0.7415	22.37

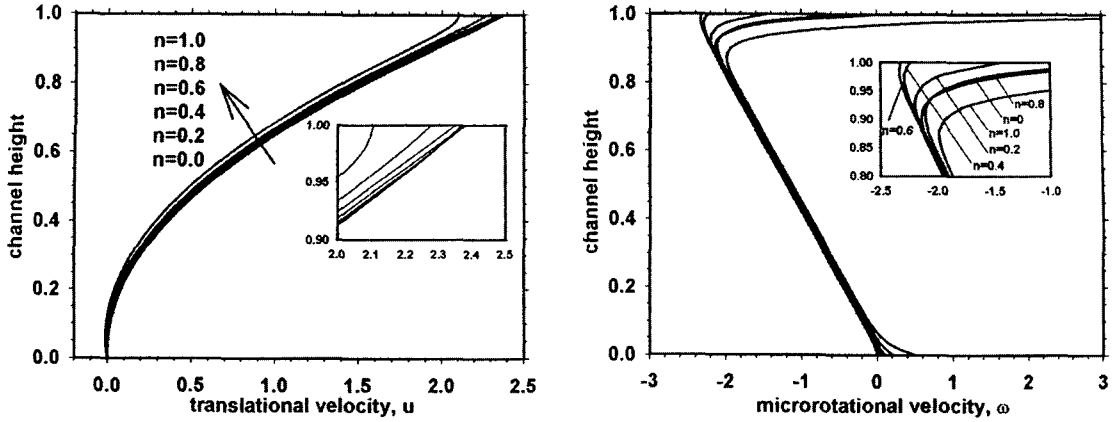

(a) Translational velocity (b) Micro-rotational velocity

Fig. 2 Effects of micro-gyration parameter n on velocity profiles for $\beta=2$, $m=0.1$, $Up=0.1$, Re=10 and $dp/dx=1$

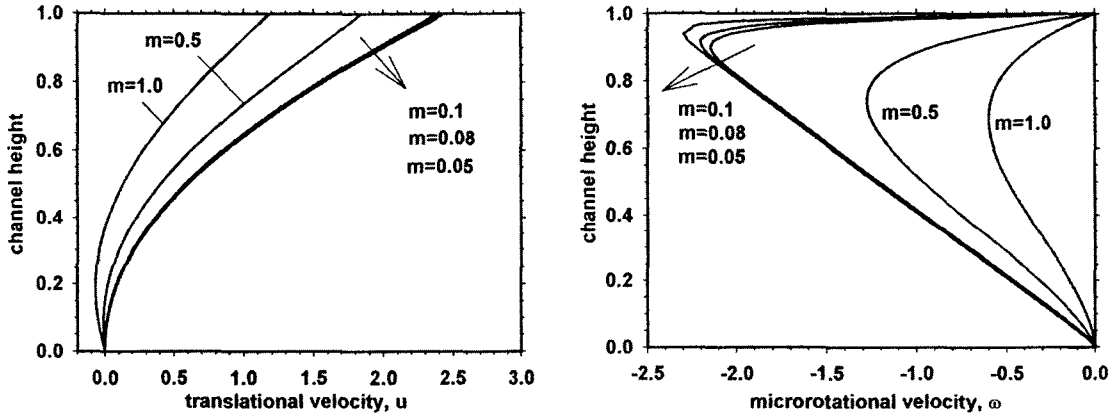

(a) Translational velocity (b) Micro-rotational velocity

Fig. 3 Effects of model parameter m on velocity profiles for $n=0$, $\beta=2$, $Up=0.1$, Re=10 and $dp/dx=1$

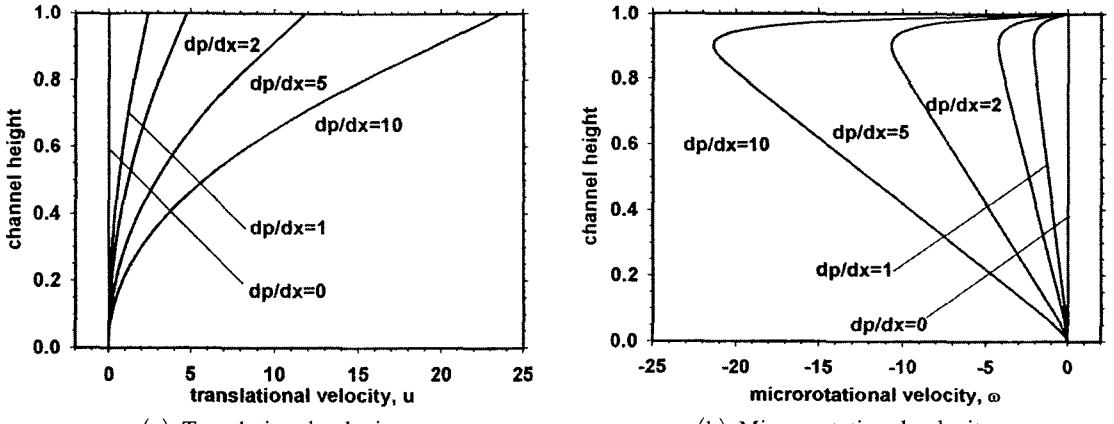

(a) Translational velocity (b) Micro-rotational velocity

Fig. 4 Effects of pressure gradient dp/dx on velocity profiles for $n=0$, $m=0.1$, $\beta=2$, $Up=0.1$ and Re=10

wise and micro-rotational velocities across the channel for various values of the pressure gradients in the direction of fluid flow, while the characteristic length ratio (m) was set to 0.1. As expected, the translational velocity increases near the upper plate as the pressure gradient increases. Also, the magnitude of micro-rotational velocity in the channel is increased as the pressure gradient increases.

The variation of skin friction coefficient for various values of the model parameter m with $n=0$, $Up=0.1$, Re=10 and $dp/dx=1$ is shown in Fig. 5. It is seen that as the β-parameter increases the skin friction coefficient at the upper plate decreases. Furthermore, an increment in m-parameter causes a decrease of the skin friction coefficient at the upper plate. However, it is noted from Table 1 that there is a maximum value on the skin friction coefficients for non-zero values of the micro-gyration boundary condition coefficient (n) with increment in β-parameter. This value can be analytically found by $dC_f/d\beta=0$.

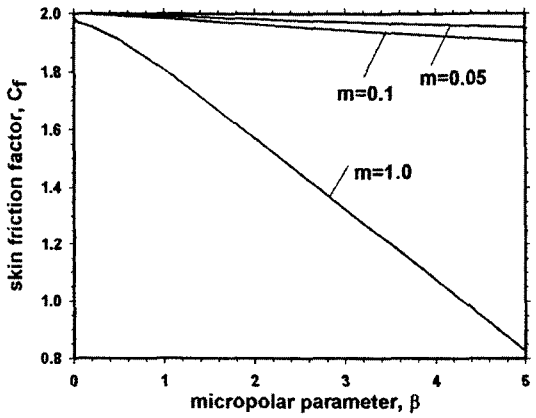

Fig. 5 Effects of micropolar parameter β on the skin friction coefficient at the upper plate for various values of model parameter m with $n=0$, $Up=0.1$, Re=10 and $dp/dx=1$

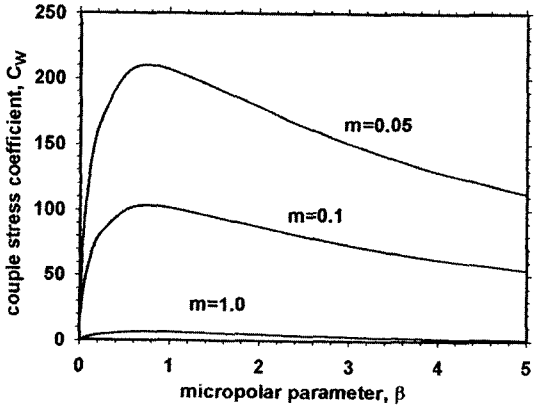

Fig. 6 Effects of micropolar parameter β on the couple stress coefficient at the upper plate for various values of model parameter m with $n=0$, $Up=0.1$, Re=10 and $dp/dx=1$

Figure 6 shows the effect of m-parameter on the couple stress coefficient at the upper plate for various values of the β-parameter. It is found that the couple stress coefficient decreases with the increase of the m-parameter. It is also noticed that for smaller m-value, the coefficient first increases up to $\beta\approx0.7$ and decreases thereafter.

4. Conclusions

In this study, a model based on micropolar fluid theory is used to examine the behavior of a plane Couette flow between two parallel plates of a viscous, incompressible, micropolar fluid. Numerical results are presented to illustrate the details of the flow characteristics and their dependence on the material parameters. The vortex viscosity to bulk viscosity ratio β was found to have much more of an impact on the flow behaviors. It is also observed that the micro-gyration boundary condition coefficient (n) influenced on the coefficients of skin friction and couple stress at the upper plate due to its different effect on the surface stress.

For better understanding of the above flow behaviors, however, it may be necessary to perform the experimental works. In the near future we would be glad to compare these analytical results with those obtained by anyone in the same field.

Acknowledgment

The authors are grateful for the financial support provided by Korea Research Foundation Grant (KRF-2002-041-D00081).

References

Ahmadi, G., 1976, "Self-Similar Solution of Incompressible Micropolar Boundary Layer Flow Over a Semi-Infinite Plate," *Int. J. Engng. Sci.*, Vol. 14, pp. 639~646.

Ariman, T., Turk, M. A. and Sylvester, N. D., 1973, "Microcontinuum Fluid Mechanics-A Review," *Int. J. Engng. Sci.*, Vol. 11, pp. 905~930.

Eringen, A. C., 1964, "Simple Microfluids," *Int. J. Engng. Sci.*, Vol. 2, pp. 205~217.

Forcada, M. L. and Mate, C. M., 1993, "The Flow of Thin Viscous Liquid Films on Rotating Disks," *J. Colloid Interface Sci.*, Vol. 169, pp. 218~225.

Jiang, X. N., Zhou, Z. Y., Yao, J., Li, Y. and Ye, X. Y., 1995, "Micro-Fluid Flow in Microchannel," *Proc. Transducers 95*, Stockholm, Sweden, pp. 317~320.

Kim, Y. -J., 1999, "A Similarity Solution of the Characteristics of Micropolar Fluid Flow in the Vicinity of a Wedge," *Trans. of KSME B*, Vol. 23, No. 8, pp. 969~977.

Papautsky, I., Brazzle, J., Ameel, T. A. and Frazier, A. B., 1999, "Laminar Fluid Behavior in Microchannels Using Micropolar Fluid Theory," *Sensors and Actuators*, Vol. 73, pp. 101~108.

Rees, D. A. S. and Bassom, A. P., 1996, "The Blasius Boundary-Layer Flow of a Micropolar Fluid," *Int. J. Engng. Sci.*, Vol. 34, pp. 113~124.

Schlichting, H., 1979, *Boundary Layer Theory*, McGraw-Hill, New York.

Yager, P. P. and Brody, P., 1996, "Low Reynolds Number Microfluidic Devices," *Proc. Solid-State Sensor and Actuator Workshop*, Hilton-head, pp. 105~108.